

Process-based indicators to assess storm induced coastal hazards

Óscar Ferreira, Theodoros A. Plomaritis, Susana Costas

CIMA/FCT, University of Algarve, Campus de Gambelas, 8005-139, Faro, Portugal;
oferreir/tplomaritis/scotero@ualg.pt

Corresponding author: Óscar Ferreira (oferreir@ualg.pt)

Abstract

Storms are responsible for several hazards (e.g. overwash, erosion, inundation) in coastal areas, leading to the destruction of property and loss of life in populated areas. Various indicators are used to express potential storm impact and describe the associated hazards. The most commonly used indicators include either forcing parameters (e.g. wave height, sea level) or coastal morphologies (e.g. dune height or berm width). Whereas they do not represent the processes associated with storm induced hazards in coastal areas. Alternatively, a hazard could be better characterised if process-based indicators are used instead. Process-based indicators express the result of the forcing mechanisms acting over the coastal morphology and reflect both hydrodynamic and morphological characteristics. This work discusses and synthesizes the most relevant process-based indicators for sandy shores subject to overwash, erosion and inundation promoted by storms. Those include: overwash depth, potential and extent; shoreline, berm or dune retreat; vertical erosion; and inundation depth and extent. The selection of a reduced set of process-based indicators to identify coastal hazards induced by storms in sandy coasts will facilitate comparison of different coastal behaviours for distinct storm return periods, and help to optimise coastal management plans, thereby contributing to the reduction of coastal risks.

Process-based indicators to assess storm induced coastal hazards on sandy coasts

Óscar Ferreira, Theocharis A. Plomaritis, Susana Costas

CIMA/FCT, University of Algarve, Campus de Gambelas, 8005-139, Faro, Portugal;
oferreir/tplomaritis/scotero@ualg.pt

Corresponding author: Óscar Ferreira (oferreir@ualg.pt)

Abstract

Storms are responsible for several hazards (e.g. overwash, erosion, inundation) in coastal areas, leading to the destruction of property and loss of life in populated areas. Various indicators are used to express potential storm impact and describe the associated hazards. The most commonly used indicators include either forcing parameters (e.g. wave height, sea level) or coastal morphologies (e.g. dune height or berm width). Whereas they do not represent the processes associated with storm induced hazards in coastal areas. Alternatively, a hazard could be better characterised if process-based indicators are used instead. Process-based indicators express the result of the forcing mechanisms acting over the coastal morphology and reflect both hydrodynamic and morphological characteristics. This work discusses and synthesizes the most relevant process-based indicators for sandy shores subject to overwash, erosion and inundation promoted by storms. Those include: overwash depth, potential and extent; shoreline, berm or dune retreat; vertical erosion; and inundation depth

and extent. The selection of a reduced set of process-based indicators to identify coastal hazards induced by storms in sandy coasts will facilitate comparison of different coastal behaviours for distinct storm return periods, and help to optimise coastal management plans, thereby contributing to the reduction of coastal risks.

Keywords: indicators; hazards; storms; overwash; inundation; erosion

1. Introduction

Storms impacting sandy coastal areas produce hazards such as erosion and inundation that, in turn, promote risk to life and property damage in occupied areas, and the alteration and/or fragmentation of habitats. Recent examples include the severe coastal erosion and associated destruction of property caused by Hercules storm (January 2014) that impacted the southwest coasts of France and England (Castelle et al., 2015; Masselink et al., 2016a,b); the inundation and loss of life caused by the Xynthia storm (February/March 2010) in western France (e.g. Bertin et al., 2012); the vast destruction caused by the superstorm Sandy (October/November 2012), in the coastal mid-Atlantic states of the USA (Bennington and Farmer, 2015; Clay et al., 2016), or by hurricane Katrina (August 2005), at the Gulf coast of the USA (Link, 2010; Kantha, 2013). Potential coastal damages and risks are expected to increase in the near future not only in association with climate change (e.g. sea level rise, change in frequency and magnitude of storms) but also due to increasing human occupation in coastal areas (Neumann et al., 2015).

119
120
121 44 Indicators, as a metric for coastal state, dynamics, behaviour or hazard, are a
122
123 45 straightforward way to express complex data and information and can therefore be an
124
125 46 important tool in the dialog among stakeholders (Carapuço et al., 2016). They are
126
127 47 often based on a parameter that is used to characterise a coastal area. Coastal hazard
128
129 48 indicators are commonly used to express the potential storm impacts in coastal areas,
130
131 49 helping to identify and prioritise vulnerable regions (Nguyen et al., 2016). Storm
132
133 50 related hazards have been expressed in the literature by a large number of different
134
135 51 indicators that have been recently synthesised by the review works of Carapuço et al.
136
137 52 (2016) and Nguyen et al. (2016). For coastal erosion and flooding hazards Carapuço et
138
139 53 al. (2016) identified (and recommended) the use of several geoindicators, like
140
141 54 *shoreline/baseline position, shoreline evolution, beach/barrier elevation or beach*
142
143 55 *slope*. Nguyen et al. (2016) synthesized the existing indicators in literature related to
144
145 56 storm surge-driven flooding and coastal vulnerability and included geoindicators (e.g.
146
147 57 *coastal slope, geomorphologic characteristics*), hydrodynamic indicators (e.g. *wave*
148
149 58 *height, tidal range, surge height*) and coastal evolution indicators (e.g. *erosion rate,*
150
151 59 *shoreline/coastline position*). The aforementioned indicators, which represent a
152
153 60 summary of the ones that have been widely used and referred to in the international
154
155 61 literature, include forcing/driver parameters, coastal morphology characteristics and
156
157 62 even coastal evolution. It is, however, not clear how to select the most representative
158
159 63 parameter for a given hazard. The most commonly used parameters describe either
160
161 64 the driving mechanisms or the coastal morphology, rarely integrating both or fully
162
163 65 representing the processes associated with storm induced hazards in coastal areas.
164
165 66 Moreover, these indicators hardly differentiate relevant time-scales (or return periods)
166
167
168
169
170
171
172
173
174
175
176
177

and/or values that are averaged over time, which can cause difficulties (and exaggerated simplicity) in their application.

To fully characterise a coastal hazard it is necessary to use a set of indicators that combines the forcing mechanism and its effect on the coastal morphology, i.e. process-based indicators. The majority of the indicators found in the literature cannot be considered process-based. Process-based indicators can only be obtained from the application of models that incorporate physical forcing mechanisms and that include realistic coastal morphology elements, resulting in a parameter or set of parameters that express the effects of the processes acting on the coastal system.

This work reviews and synthesizes the most relevant process-based coastal indicators that can be applied for sandy coasts subject to storm-induced coastal hazards. The main hazards assessed are: overwash, inundation, and erosion. The main goal is to propose a set of process-based indicators that can serve as a reference for coastal hazard studies on sandy shores. The rationale for using process-based indicators is described in section 2. The definition, discussion and selection of indicators for each analysed coastal hazard are detailed in section 3. Section 4 provides a synthesis of the proposed indicators and their applicability, based on the use of simple parameters highly representative of coastal hazards. Final considerations on current limitations and future use of process-based indicators at sandy coasts are discussed in section 5.

2. Process-based indicators

237
238
239 88 The vast majority of recommended coastal hazard related indicators in the literature
240
241 89 (see reviews by Bush et al., 1999; Carapuço et al., 2016; Nguyen et al., 2016) only take
242
243 90 into account: (i) the characteristics of the physical/morphological features of the
244
245 91 coastal system, or (ii) the driving mechanism. Combinations between both,
246
247 92 representing the processes and the consequent hydrodynamic or morphological
248
249 93 results (process-based indicators), are not commonly used and have not yet been the
250
251 94 subject of a synthesis. Process-based indicators are directly related to hazard and
252
253 95 represent the interaction between driving mechanisms and the coastal morphology.
254
255 96 The process-based indicators are therefore obtained by using formulations or models
256
257 97 (from simple to complex) that will combine the driving mechanisms (e.g. storm
258
259 98 parameters like wave height, wave period, storm duration or sea level) and the coastal
260
261 99 system morphology (such as beach face slope, dune height, berm width, grain size or
262
263 100 bathymetry) (Figure 1, steps 1 and 2). The result will be an impact (e.g. erosion,
264
265 101 overwash occurrence) that can be expressed through an indicator that has a physical
266
267 102 meaning (e.g. flood depth, shoreline retreat). Overall, results can be reclassified into
268
269 103 new classes that express different levels of hazard according to stipulated
270
271 104 limits/thresholds allowing an illustrative mapping of the hazard (Figure 1, steps 3 and
272
273 105 4). These thresholds can be defined locally or regionally, allowing a comparison of the
274
275 106 hazard intensity within a specific coastal area and also between different coastal areas.
276
277 107 Furthermore, such indicators can often be used to estimate (or to indicate) the extent
278
279 108 of the hazards, allowing the representation of the spatial distribution of the coastal
280
281 109 hazard. However, it is worth mentioning that the thresholds depend on the hazard
282
283 110 receptor-type (e.g. dunes, salt marsh, houses, infrastructure), defined according to the
284
285 111 Language of Risk (Gouldby and Samuels, 2005) and, therefore, comparisons should be
286
287
288
289
290
291
292
293
294
295

restricted to similar receptors. These indicators are comparable in concept to the Coastal State Indicators (CSI), introduced by van Koningsveld et al (2005). CSI are defined as “issue-related parameters that can simply, adequately and quantitatively describe the dynamic-state and evolutionary trends of a coastal system” (Davidson et al., 2006, 2007). The use of process-based indicators can therefore include alongshore and cross-shore variability as well as time-dependency (e.g. inclusion of time-scales or return periods). The indicators must, however, remain simple on application and expression to ensure their applicability by most coastal managers. Examples of commonly used process-based indicators (e.g. Wright and Short, 1984 or Masselink and Hegge, 1995) include beach morphodynamic state indicators such as the surf scaling parameter (Guza and Inman, 1975) and the surf similarity parameter (Battjes, 1974). However, these are not commonly applied to indicate the degree of coastal hazard. In fact, widely accepted process-based indicators to represent storm hazard at sandy coasts have not yet been defined and used.

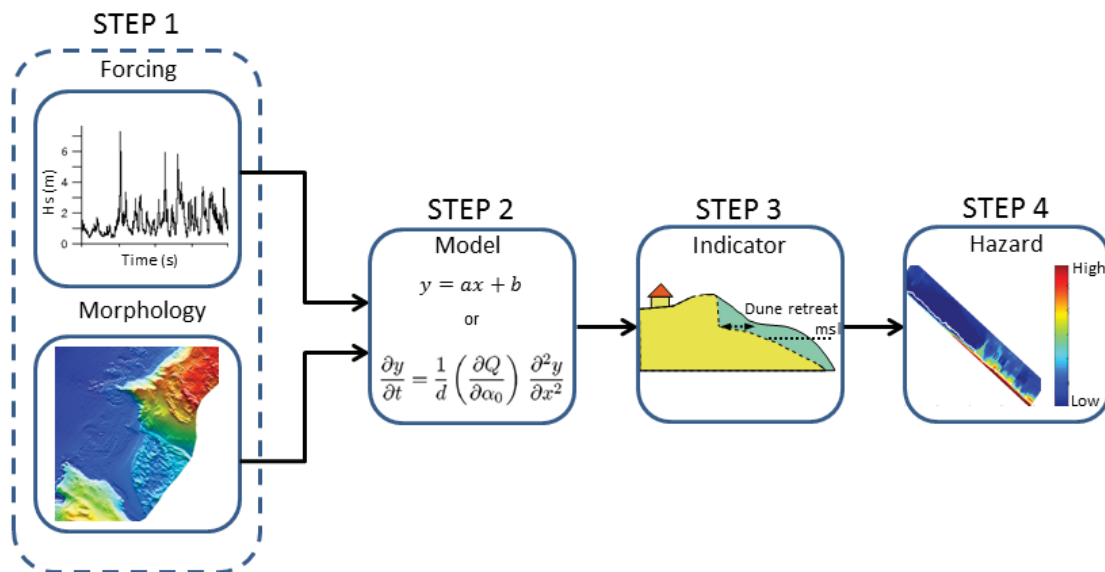


Figure 1. Scheme representing the steps needed to obtain a process-based indicator, and its use for hazard assessment. Driving mechanisms and coastal morphology (Step 1) are integrated in numerical models (from simple to complex) to produce a process-based indicator (step 3) that can be used to express the hazard degree (step 4). Two possible approaches can be used to obtain the indicator's variability through time: event approach and response approach (see Divory and McDougal, 2006; Bosom and Jiménez, 2011; Ferreira et al., 2016). The *event approach*, also called deterministic, uses the extreme probability distribution of the physical forcing parameter and the present day coastal morphology (or any simulated condition) to determine the process-based indicator. The storm parameter (e.g. wave height) for a given return period is obtained from the corresponding extreme distribution. A formulation/model (Step 2 on Figure 1) is then applied for the dominant (or other) morphological condition and the process-based indicator is obtained (e.g. overwash depth, shoreline retreat) for that return period. In this approach the obtained indicator is then associated with one value of a storm parameter, for a given return period, losing significant information on the natural variability of the process (Sánchez-Arcilla et al., 2009). The *response approach*, also called the probabilistic approach, uses the entire forcing parameter time-series (e.g. water level, wave height, storm duration) to obtain the indicators for all known conditions (e.g. runup, erosion) through time. A probability distribution of extremes must be fitted to the obtained indicator time-series and the indicator associated with a given return period will be computed from its own probability distribution. This method is particularly recommended when the forcing variables are poorly correlated or statistically independent (Bosom and Jiménez, 2011).

3. Proposed process-based indicators

A large number of the indicators that are currently used are frequently poorly defined (Carapuço et al., 2016). The existing lack of standardization of concepts and assumptions restricts the comparability between indicators and among different coastal areas (Nguyen et al., 2016). The use of different indicators may even result in significantly different hazard estimates, requiring greater caution in the selection of the appropriate indicators (Hanslow, 2007). All above expressed shortcomings call for a standardized approach, with clear guidelines for the determination and applicability of hazard indicators. Indicators should, therefore, be as simple as possible, unambiguous, reproducible in different coastal regions, and based on a consistent methodology that enables comparison between sites (see Carapuço et al., 2016; Nguyen et al., 2016). Moreover, they should be suitable for defining the morphodynamic and hydrodynamic state of sedimentary coasts, in support of coastal zone management (Davidson et al., 2006).

The indicators analysed in this paper are process-based and therefore describe the dynamic interaction between the coastal morphological states and the driving mechanisms of the particular hazard. The computation of the proposed indicators for existing (or hindcast) data time-series, and subsequent probabilistic analysis of the indicators' distribution, will allow their use in association with return periods. Since the selected indicators are applicable to sandy coastal areas and can be associated with a given probability of occurrence, they allow direct comparisons or ranking of the hazard intensity between different coastal areas. For each indicator a set of thresholds can be

established (at local, regional or international level) that can be used to classify and rank the hazard. Those limits will not be the subject of detailed analysis in this paper, although application examples will be mentioned after the physical description of each indicator.

Overwash indicators

Overwash occurs when wave induced runup overtops the foredune ridge or the highest beach/barrier elevation if the dune is absent. Following Matias and Masselink (2017) the overwash is a discontinuous flow of seawater and sediment over the dune/beach crest, which will propagate inland for a given extent (distance to the initial dune/beach crest position). The two main indicators reflecting overwash induced hazards are: *overwash potential* and *overwash depth*. Overwash potential is defined as the vertical difference (in meters) between the potential wave runup (along an imaginary extended beach/dune slope) and the dune/beach crest elevation (Matias et al., 2012, 2016; Figure 2). Overwash depth can be defined (adapted from Donnelly, 2008) as the water depth (in meters) at a point (dune crest or backbarrier) during an overwash event. Overwash depth decreases with the distance across the backbarrier until reaching a zero value at the maximum inland overwash extent (Figure 2). Computation of both indicators requires the use of empirical equations to predict the runup (e.g. Holman, 1986; Stockdon et al., 2006; see Matias et al., 2012 for a review on formulations) and a digital terrain model. For complex environments, such as partially engineered coastlines or areas with a complex geomorphological framework, process-based models should be used to determine such indicators.

Both indicators (overwash potential and overwash depth) state a vertical difference between a water level associated with the overwash and the terrain (Figure 2). The overwash potential is easier to use because of its computational simplicity since it compares the result of a runup formulation with the height of the dune/berm crest. The overwash depth needs extra formulations to determine the effective water lens depth at the crest and its cross-shore variability (see Donnelly, 2008). However, the overwash depth has the advantage of being physically representative of the actual process as it can be applied not only at the dune/beach crest but also at the backbarrier up to the maximum extent of the overwash (Figure 2). The computation of the overwash depth can be performed using the formulations proposed in Donnelly (2008), relating the overwash depth with infiltration and the velocity of the overwash flux. However, this approach has not been calibrated for all grain-sizes and assumes a simplified morphology. Overwash depth values at the back of the dune can be estimated by using an exponential decay that varies according to infiltration and lateral expansion of the flow. This also allows the definition of a maximum *overwash extent* which represents the total cross-shore extension of the overwash and can be applied as an indicator of the area prone to be flooded (e.g. Garcia et al., 2010; Ferreira et al., 2016; Christie et al., 2017). The inclusion of processes like infiltration and lateral expansion increases the applicability of the method by providing free parameters that can be set to local conditions and used as calibration parameters. A more effective (but also more complex and computationally demanding) way to compute the overwash depth is to use 1D or 2D numerical models. Other potential indicator to state the overwash hazard (for expected damages) is the overwash velocity. This is currently obtained (with limited field validation) by using models and it is therefore of restricted

application. Alternatively, the overwash velocity can be estimated as a function of the overwash depth at the dune crest, as determined by Donnelly (2008) and Matias et al. (2016).

Existing studies mostly use the overwash depth and the overwash potential to determine the possibility of overwash for a given event. Negative values of these indexes are associated with swash or collision states, according to the storm impact scale proposed by Sallenger (2000), while positive values imply overwash (e.g. Almeida et al., 2012; Rodrigues et al., 2012) or higher hazard levels such as inundation (e.g. Bosom and Jiménez, 2011). Several researchers have applied the overwash potential indicator in order to find a storm threshold for morphological changes (e.g. Stockdon et al., 2007; Almeida et al., 2012; Armaroli et al., 2012; Del Río et al., 2012; Haerens et al., 2012; Trifonova et al., 2012). The use of the overwash depth is still limited (e.g., Ferreira et al., 2016; Poelhekke et al., 2016; Valchev et al., 2016; Christie et al., 2017) since it is not directly obtained by the most commonly used formulas (e.g. Holman, 1986; Stockdon et al., 2006) and has been rarely measured in the field, leading to lack of validation. However, it has to be stated that overwash depth is a measurable value in the field in contrast with the overwash potential. For gravel barriers and laboratory conditions, such measurements have been obtained by Matias et al. (2011) as a result of the Bardex Project (Williams et al., 2009). Future application of the overwash depth and overwash potential values should be based on severity scales, to be developed at local, regional or even international levels, as a function of the potential hazard associated with each overwash level. Specific depth damage curves can then be obtained to assess the risk associated with overwash such as already exists for riverine floods.

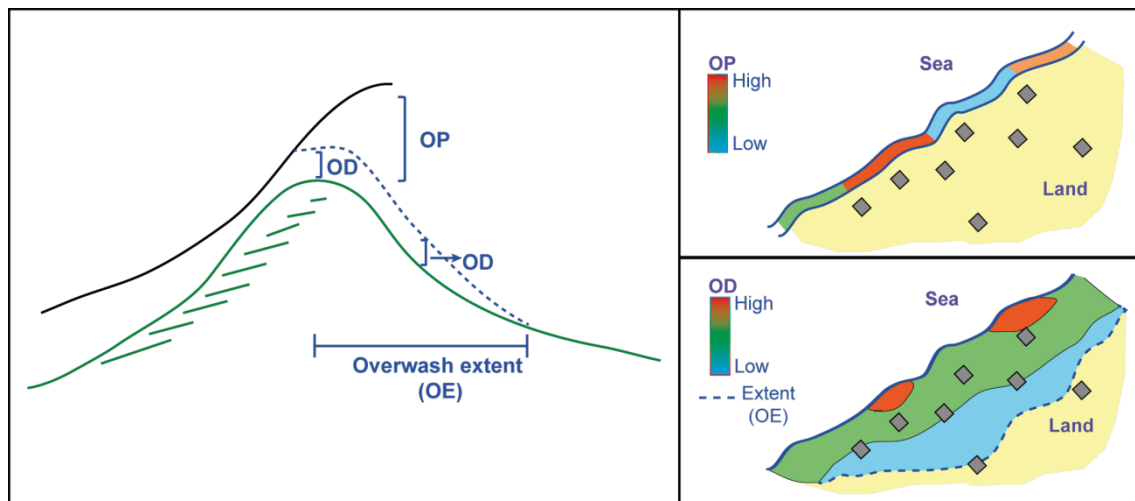


Fig 2. Cross-shore and plan view representing the concept and application of overwash indicators. Grey squares represent the location of the hazard receptors (e.g. houses). OD – overwash depth; OP – overwash potential; OE – overwash extent.

Inundation indicators

Inundation, which is here defined according to the concept proposed by Sallenger (2000), occurs when the storm related still water level (tide + surge) is sufficient to completely and continuously submerge a barrier (i.e. the dune crest or the highest barrier elevation). Inundation should not be confused with overwash, were an intermittent runup level overpasses the barrier for short periods (seconds), and must be treated separately as different time (hours to days) and spatial (larger areas and depths) scales are involved. Important processes for tide/surge interactions that can affect the water level (surge height) are surge propagation during the tidal cycle and wind forcing. The continental shelf depth and width are important factors on the amplification (mainly for shallow and wide shelves) of both processes (see Fortunato et al., 2016). Finally, the storm trajectory and the timing of the storm affect the total

water level (Bertin et al., 2012). For small areas, the total water level can be assumed constant but when the inundation affects very large areas a variable level could be applied (Breilh, et al., 2014).

The extent of the inundation can be determined through several methods with different degrees of complexity. A simple bathtub model approach can be used for areas with low morphological complexity (Figure 3). In this method, a given area becomes inundated if its elevation is less than the water level (Poulter and Halpin, 2008) while a vertical water depth can be computed at each point. The method does not account for infiltration, roughness or shear stress and therefore it can lead to overestimation. An adaptation can be performed in order to reduce the level of error on the estimation of the inundated area and water depth by using a tilted water surface (Figure 3) along a sloping plane (see Sekovski et al., 2015) based on historical information and cartography. Problems arise from the application of this simple methodology when the total inundated area is large and therefore the time needed to achieve complete inundation is too long when compared with the actual flooding time. This is particularly valid in inundation areas subjected to tides, where the inundation level can occur for just a few hours. In such cases, more complex methods, such as the flood intensity index (Dottori et al., 2016) should be applied. This index reproduces flooding processes using as theoretical background the 1D uniform flow equation, and considers the vertical differences between the water level at a given source of the flow and the elevation of the adjacent terrain. Inundation models, such as LISFLOOD (De Roo et al., 2000), which can account for lateral connectivity and permeability, can also be used to better represent the inundation area and depth. The main indicator to be used on hazard assessment should be the *flood depth* (see Figure 3) at each hinterland

position, which expresses the intensity of the hazard and its variability along each considered coastal region. Other useful indicators worth of mentioning are the *total flood extent* (see Figure 3) from a given reference point (e.g. the shoreline), and the *percentage of flooded area per coastal sector* (from the shoreline to a given previously defined hinterland limit). The *overflowing discharge volume* can also be used. This indicator is a function of the overflow depth at the crest of a dune or dyke multiplied by its length and integrated over time using the rectangular weir discharge equation of Kindsvater and Carter (1957). The extension of the overflowing discharge volume can be calculated by a step by step increase in the water level until the total volume is reached. Similarly, the volume can be used in combination with the tilting bathtub method to compare inundation volumes.

An example of the application of the tilted bathtub method can be found in Sekovski et al. (2015). The authors used both the flood depth (total water level at a given point) and the flood extent to evaluate present-day and future flood hazards at coastal cities from Emilia-Romagna (Italy). An inter comparison of the above methods to assess the inundation caused by the Xynthia storm to La Faute-sur-Mer is provided by Breilh et al. (2013) and Vousdoukas et al. (2016). Furthermore, Vousdoukas et al. (2016) applied the above indicators to assess the flood hazard along the entire European coast. Poulter and Halpin (2008) used and improved the bathtub method by incorporating the hydrological connectivity between grid cells by considering that only cells that have a connection with the open sea or with nearby cells are considered flood-prone. Perini et al. (2016) used the tilted bathtub approach and the Cost Distance tool of ArcGIS to produce a least-path cost analysis and to remove isolated areas without hydrological connectivity in order to improve the final flood maps.

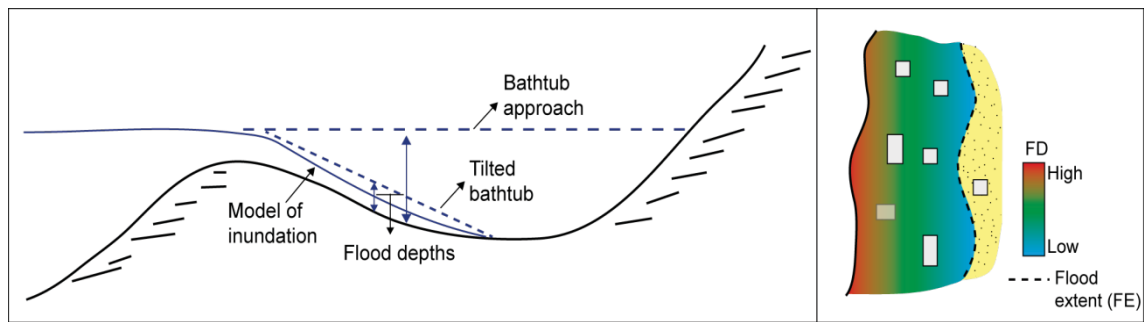


Fig 3. Cross-shore and plan view representing the concept and application of the inundation indicators. White polygons represent the location of the hazard receptors (e.g. houses, hotels). FD – Flood depth; FE – Flood extent.

Erosion indicators

Erosion in this paper simply refers to short-term (episodic) effects driven by storm events or storm groups effecting coastal areas, excluding continuous erosion caused by persistence of sediment scarcity. Storm-induced erosion can be observed as a vertical lowering of the beach/dune system (or by scarp or bluff formation, including subsequent dune avalanching) or as a horizontal inland displacement of the coast (e.g. barrier rollover). The erosion associated with storms will not necessarily result on an overall and definitive displacement of the shoreline since the coast can recover to its original configuration if there is enough sediment available. However, the promoted vertical and horizontal shifts are capable of producing destruction and damages if occupation or other receptors are present. Three main indicators can be proposed: *shoreline/berm retreat*, *dune foot retreat*, and *vertical erosion* (all in meters) at a given point (e.g. dune foot, dune crest, at the infrastructure) (Figure 4). The shoreline/berm retreat and the dune foot retreat represent the horizontal displacement produced by

the storm at a given coastal feature (Figure 4), and can be directly compared with occupation to assess vulnerability. The use of the shoreline/berm retreat versus the dune foot retreat as indicators depends very much on the exposed elements to be assessed. For coastal areas with infrastructure located on the beach berm or on the beach face (e.g. bars, amenities) the shoreline/berm retreat should be used, which can then be transformed (or not) into a remaining beach width or into a distance to occupation. For coastal areas where development and infrastructure (e.g. houses, roads) are located on the dune or at the hinterland, the dune foot retreat should be applied. This can also be transformed into a remaining distance to the developed area when necessary/applicable. The use of the shoreline/berm retreat versus the dune foot retreat also depends on the coastal morphology; at sandy coasts without a dune the shoreline/berm retreat should be used. The vertical erosion corresponds to the vertical difference between the original morphology and the computed/observed morphology during and after the storm (Figure 4). Vertical differences can result in potential damage for the existing development on the beach. This indicator can be equally used on the berm, dune or backbarrier, for any storm and given morphological characteristics, allowing the cross-shore determination and comparison of the vertical erosion indicator. The retreat/erosion indicators can be computed by using relatively simple analytical models, such as the convolution model (Kriebel and Dean, 1993), Larson's method (Larson et al., 2004), the erosion structural function (Mendoza and Jiménez, 2006), or the ShoreFor behaviour model (Davidson et al., 2013), among many others. These models use relatively simple analytical formulations that integrate driving mechanisms (such as wave height, storm duration and sea level) jointly with the morphological and sedimentological characteristics of the coastal area (e.g. dune

height, berm width, beach slope or grain size) to determine coastal erosion (volume or retreat) induced by each storm. All the above methods deal with swash and collision conditions but not with overwash and inundation. For the later regimes, the erosion processes are different and generally more complex. Process-based models, like XBeach (Roelvink et al., 2009), can also be employed to determine the same indicators, for all regimes and with greater detail but requiring a higher level of computational complexity and available data for model calibration. Process-based models like XBeach reproduce the processes occurring at coastal areas during a storm, containing the essential physics of dune erosion, overwash, avalanching, swash, infragravity waves and wave groups (Roelvink et al., 2009). Finally, if LIDAR (Light Detection and Ranging) or similar resolution/quality data (e.g. from UAVs or satellite imagery) exists for pre- and post-storm conditions the erosion indicators can also be computed based on direct measurements (for example by comparing pre and post storm digital terrain models) and for all storm impact regimes following the method of Stockdon et al. (2007).

According to Ciavola et al. (2015) dune erosion volume, berm retreat or dune height reduction can be used directly or against thresholds to identify areas prone or resistant to erosion hazards. Nevertheless, the use of process-based erosion indicators is not widespread, with trend indicators such as shoreline position, high water line, vegetation line or scarp location (see Hanslow, 2007) being the most widely used. The sub-aerial beach and dune volume are also used as coastal indicators (Hanslow, 2007; Armaroli et al., 2012) but not necessarily as process-based indicators, with exceptions such as the use of the erosion resistance index by Judge et al. (2003), the eroded volume and the beach retreat (e.g. Mendoza and Jiménez, 2006), and the dune

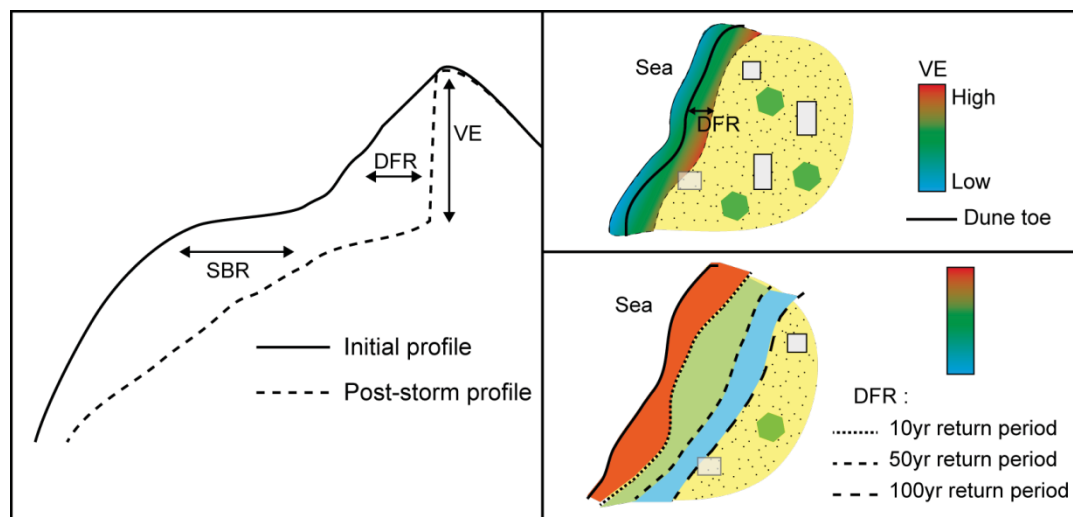


Fig 4. Cross-shore and plan view representing the concept and application of the erosion indicators. White polygons represent the location of the hazard receptors (e.g. houses, hotels). SBR – Shoreline/Berm retreat; DFR – Dune foot retreat; VE – Vertical erosion.

4. Summary of indicators and discussion of use

A synthesis of the reviewed and proposed indicators for three main analysed hazards (overwash, inundation and erosion), on sandy shores, can be found in Table I. The proposed process-based indicators are all simple in concept and refer to a measurable distance, permitting a cartographic expression of the hazard (see figures 2 to 4). Several indicators report a vertical difference to the initial topographic surface

1063
1064
1065
1066
1067
1068
1069
1070
1071
1072
1073
1074
1075
1076
1077
1078
1079
1080
1081
1082
1083
1084
1085
1086
1087
1088
1089
1090
1091
1092
1093
1094
1095
1096
1097
1098
1099
1100
1101
1102
1103
1104
1105
1106
1107
1108
1109
1110
1111
1112
1113
1114
1115
1116
1117
1118
1119
1120
1121

392 (overwash depth, overwash potential, flood depth, vertical erosion) representative of
393 an interaction between driving processes (e.g. water level, runup) and such surface (as
394 is the case for overwash depth, overwash potential and flood depth) or the result of
395 the morphodynamic process measured as a difference between pre and post-event
396 surfaces (vertical erosion). Others (overwash extent, flood extent, shoreline/berm
397 retreat, and dune foot retreat) register the cross-shore extent of the hazard. The
398 alongshore integration of both (vertical and horizontal indicators) allows, in most
399 cases, for an overall three-dimensional cartography of the hazard, including the
400 potentially affected areas and the vertical level of action. That is, for instance, the case
401 of the joint use of the overwash/flood depth and the associated extent. The vertical
402 erosion indicator, since it is immediately associated with an inland position, allows a
403 direct three-dimensional representation of the hazard when expressed alongshore.

404 The here-reviewed and proposed indicators can be applied on natural sandy (or
405 gravely) beaches with or without dune systems or backbarriers. Although the
406 indicators are not necessarily limited in their use, some of the proposed approaches
407 are, and they can only be applied to coastal areas with low morphological complexity.

408 This includes the case of the determination of the flood depth/extent by using a
409 bathtub (or tilted bathtub) approach. Most of the existing formulations and models are
410 also not completely adapted to heavily developed hinterlands (e.g. dominated by
411 impermeable surfaces) and will require some adaptation. Previous knowledge of the
412 dominant processes during storms will also help to correctly select the methods and
413 indicators to use in the most cost-effective way.

1122
1123
1124
1125
1126
1127
1128
1129
1130
1131
1132
1133
1134
1135
1136
1137
1138
1139
1140
1141
1142
1143
1144
1145
1146
1147
1148
1149
1150
1151
1152
1153
1154
1155
1156
1157
1158
1159
1160
1161
1162
1163
1164
1165
1166
1167
1168
1169
1170
1171
1172
1173
1174
1175
1176
1177
1178
1179
1180

414 A direct comparison on the applicability of selected (based on the works of Carapuço
415 et al., 2016 and Nguyen et al., 2016) geo- and driver- based indicators against the
416 proposed process-based indicators is expressed at Table II. Most geo- and driver-based
417 indicators are easier to obtain since they can be directly extracted from existing
418 cartography or field measurements (geoindicators) and from instrumental
419 measurements or hindcast predictions (driver-based indicators) often available on-line.
420 They are commonly converted into several simple semi-quantitative values (e.g. from 1
421 to 5) that are added (quantified) alongshore to permit a representation of the hazard,
422 making them simple to use even for non-experts. They are therefore still used as a
423 simple methodology to classify the coast according to its vulnerability (e.g. Jiménez et
424 al., 2016). They do not, however, account for the acting processes and can therefore
425 affect the final results as observed by Judge et al. (2003) when considering the crest
426 height as a predictor of dune vulnerability. Process-based indicators require both geo-
427 and driver-based information and the additional use of formulations/models, to obtain
428 a final value. If using return periods, a statistical analysis (for either the event or
429 response approach) is also required. This implies, from the users, a higher expertise on
430 coastal dynamics, including the perception of the physical processes acting in coastal
431 areas and responsible for hazards. This reduces the applicability of process-based
432 indicators to users with sufficient background on coastal dynamics. Process-based
433 indicators have, however, several advantages that will, most probably, increase their
434 future use. Most indicators have the possibility of including both detailed longshore
435 variability and cross-shore expression of the hazard, while driver-based indicators have
436 a reduced representativeness of the longshore variability, mainly if wave propagation
437 models are not used. Most used geo and driver-based indicators are also not able to

1181
1182
1183
1184
1185
1186
1187
1188
1189
1190
1191
1192
1193
1194
1195
1196
1197
1198
1199
1200
1201
1202
1203
1204
1205
1206
1207
1208
1209
1210
1211
1212
1213
1214
1215
1216
1217
1218
1219
1220
1221
1222
1223
1224
1225
1226
1227
1228
1229
1230
1231
1232
1233
1234
1235
1236
1237
1238
1239

438 include the cross-shore expression of the hazard (with the exception of the erosion
439 rate).

440 Geo- and driver-based indicators when used alone are often site-specific and hardly
441 comparable between coastal areas. Process-based indicators present an outcome that
442 can be easily compared among sites. For instance, the vertical expression of a hazard
443 (e.g. flood depth or overwash depth) can be compared between coastal regions with
444 similar settings and a higher value of the indicator will represent a potentially higher
445 hazard. That is not the case for driver-based indicators, for instance. A higher wave
446 height or water level cannot be compared between coastal areas since the hazard will
447 depend on the relationship with the coastal elevation. A lower value of a driver-based
448 indicator can be responsible for a higher hazard if the coastal elevation is low, and the
449 opposite is also valid. This prevents the compared use of geo- and driver-based
450 indicators to assess the hazard for distinct coastal areas. The extensive use of process-
451 based indicators, for different coastal regions will allow, in the future, the
452 development of hazard levels/scales that can be internationally adopted. Since
453 process-based indicators can be associated with a given probability of occurrence and
454 can be directly compared between coastal regions, they can also be used to rank the
455 hazard intensity for vast coastal areas, for equal return periods. It must however be
456 stressed that, for the moment, no universal application of indicators exists and that
457 there are no internationally widely accepted intervals to classify each indicator
458 according to the potential hazard. This is still work to be performed, to be based on the
459 lessons learned from the application of process-based indicators at a large-scale.

The here proposed process-based indicators do not integrate feedback mechanisms resulting from the interaction between morphology and forcing agents (e.g. waves, currents). That is also the case for geoindicators and for indicators solely based on driving mechanisms. The hazard and consequent risk can change as a result of feedback mechanisms. For instance, the lowering of a dune by overwash will increase the overwash potential and the overwash depth, leading to an increase in the hazard when compared with the initial (and considered) situation/morphology. The feedback mechanism can occur differently alongshore, as a function of the nearshore, shoreface and dune morphologies. In cases where feedback mechanisms may be highly relevant, these (and other indexes) may not fully reflect the impacts associated with a given event. In those cases only process-based models with high resolution topobathymetric grids, after validation and calibration, may be helpful to better understand the hazard in coastal areas. It must be also kept in mind that the indicators must remain simple in concept and application to ensure their use by most coastal managers. Highly complex indicators requiring extreme computational effort and a high degree of specialization will probably fail to be widely applied by most coastal end-users, including managers.

5. Conclusions, limitations and future improvements

The current use of process-based indicators is still on its infancy, being necessary to establish a set of the most relevant indicators that can better express potential hazards at sandy (and gravelly) shores:

- Overwash: overwash depth, potential and extent;

1299
1300
1301
1302
1303
1304
1305
1306
1307
1308
1309
1310
1311
1312
1313
1314
1315
1316
1317
1318
1319
1320
1321
1322
1323
1324
1325
1326
1327
1328
1329
1330
1331
1332
1333
1334
1335
1336
1337
1338
1339
1340
1341
1342
1343
1344
1345
1346
1347
1348
1349
1350
1351
1352
1353
1354
1355
1356
1357

- 483 • Inundation: flood depth and extent;
 - 484 • Erosion: shoreline/berm and dune foot retreat, and vertical erosion.
- 485 The future use of process-based indicators to quantify coastal hazards is
- 486 recommended, mainly when compared to the most classical and commonly used geo-
- 487 and driver-based indicators, since they allow:
- 488 a) better quantification of the hazard by representing the interaction between
 - 489 forcing mechanisms and morphology;
 - 490 b) better expression of the alongshore and cross-shore (extent) variability of the
 - 491 hazard, including its three-dimensional representation (longshore, cross-shore
 - 492 and vertical); and
 - 493 c) comparison between coastal areas.
- 494 The development of the process-based indicators' potential will rely on their
- 495 generalised use in the future. Only an increase in their use will allow the definition of
- 496 common hazard levels for distinct coastal regions and a large-scale application to vast
- 497 areas (e.g. at pan-European level). A few limitations still exist that prevent the wider
- 498 use of these indicators. These include:
- 499 i) limited available quality data for several regions, regarding either
 - 500 morphologic and hydrodynamic parameters, which is particularly relevant
 - 501 when long-term time-series (e.g. wave characteristics) are needed to better
 - 502 define return periods;
 - 503 ii) restricted current use of formulations and models by end-users and namely
 - 504 coastal managers;

1358
1359
1360
1361
1362
1363
1364
1365
1366
1367
1368
1369
1370
1371
1372
1373
1374
1375
1376
1377
1378
1379
1380
1381
1382
1383
1384
1385
1386
1387
1388
1389
1390
1391
1392
1393
1394
1395
1396
1397
1398
1399
1400
1401
1402
1403
1404
1405
1406
1407
1408
1409
1410
1411
1412
1413
1414
1415
1416

505 iii) reduced possibility of integrating feedback mechanisms, with the exception
506 of the most complex process-based models.

507 The first limitation will be solved (with time) by the ongoing and increasing
508 improvement on data access (and quality) worldwide, including on-line access to
509 coastal morphology and wave/water level series. To obviate the second limitation an
510 improvement will be needed on the transfer of knowledge from the coastal scientific
511 community towards coastal end-users. The third limitation will be solved by integrating
512 process-based models into user-friendly frameworks for generalised use. The
513 improved and generalised use of process-based indicators will provide coastal
514 managers with a highly relevant tool to evaluate coastal hazards and risks and,
515 therefore, to better establish and implement disaster risk reduction in the future, in
516 the most cost-effective way.

517

518 Acknowledgments

519 This work was supported by the European Community's 7th Framework Programme
520 through the grant to RISC-KIT ("Resilience-increasing Strategies for Coasts – Toolkit"),
521 contract no. 603458, and by contributions by the partner institutes. Susana Costas
522 research is funded through the "FCT Investigator" program (ref. IF/01047/2014). This
523 work was also supported by the Portuguese Science Foundation (FCT) through the
524 grant UID/MAR/00350/2013 attributed to CIMA/University of Algarve

525

526 References

- 1417
1418
1419 527 Almeida, L.P., Ferreira, O., Taborda, R., 2011. Geoprocessing tool to model beach
1420
1421 528 erosion due to storms: application to Faro beach (Portugal). *Journal of Coastal*
1422
1423 *Research*, SI 64, 1830-1834.
1424 529
1425
1426
1427 530 Almeida L. P., Vousedoukas M. V., Ferreira O., Rodrigues, B.A., Matias, A., 2012.
1428
1429 531 Thresholds for storm impacts on an exposed sandy coastal area in southern Portugal,
1430
1431 532 *Geomorphology*, 143, 3-12. DOI: 10.1016/j.geomorph.2011.04.047
1432
1433
1434 533 Armaroli, C., Ciavola, P., Perini, L., Calabrese, L., Lorito, S., Valentini, A., Masina, M.,
1435
1436 534 2012. Critical storm thresholds for significant morphological changes and damage
1437
1438 along the Emilia-Romagna coastline, Italy. *Geomorphology*, 143, 34-51.
1439 535
1440 DOI: 10.1016/j.geomorph.2011.09.006
1441 536
1442
1443
1444 537 Battjes, J.A., 1974. Surf similarity. *Coastal Engineering*'74, 446-480.
1445
1446
1447 538 Bennington, B. and Farmer, E.C., 2015. *Learning from the impacts of Superstorm Sandy*.
1448
1449 539 Ed. J. Bret Bennington and E.Christa Farmer. Academic Press. Elsevier, 123 p.
1450
1451
1452 540 Bertin, X., Bruneau, N., Breilh, J.F., Fortunato, A.B., Karpytchev, M., 2012. Importance
1453
1454 541 of wave age and resonance in storm surges: The case Xynthia, Bay of Biscay. *Ocean*
1455
1456 542 *Modelling*, 42, 16-30. DOI: 10.1016/j.ocemod.2011.11.001
1457
1458
1459 543 Bosom, E. and Jiménez, J.A., 2011. Probabilistic coastal vulnerability assessment to
1460
1461 544 storms at regional scale - application to Catalan beaches (NW Mediterranean). *Natural*
1462
1463 545 *Hazards and Earth System Sciences*, 11, 475-484. DOI: 10.5194/nhess-11-475-2011
1464
1465
1466
1467 546 Breilh, J.F., Chaumillon, E., Bertin, X., Gravelle, M., 2013. Assessment of static flood
1468
1469 547 modeling techniques: application to contrasting marshes flooded during Xynthia
1470
1471
1472
1473
1474
1475

- 1476
1477
1478 548 (western France). *Natural Hazards Earth Systems Science*, 13, 1595-1612.
1479
1480 549 DOI:10.5194/nhess-13-1595-2013
1481
1482
1483 550 Bush, D.M., Neal, W.J., Young, R.S., Pilkey, O.H., 1999. Utilization of geoindicators for
1484
1485 551 rapid assessment of coastal-hazard risk and mitigation. *Ocean and Coastal*
1486
1487 552 *Management*, 42, 647-670. DOI: 10.1016/S0964-5691(99)00027-7
1488
1489
1490 553 Callaghan , D.P., Nielsen, P., Short, A., Ranasinghe, R., 2008. Statistical simulation of
1491
1492 554 wave climate and extreme beach erosion. *Coastal Engineering*, 55(5), 375-390.
1493
1494 555 DOI:10.1016/j.coastaleng.2007.12.003
1495
1496
1497 556 Carapuço, M.M., Taborda, R., Silveira, T.M., Psuty, N.P., Andrade, C., Freitas, M.C.,
1498
1499 557 2016. Coastal geoindicators: Towards the establishment of a common framework for
1500
1501 558 sandy coastal environments. *Earth-Science Reviews*, 154, 183-190. DOI:
1502
1503 559 10.1016/j.earscirev.2016.01.002
1504
1505
1506 560 Castelle, B., Marieu, V., Bujan, S., Splinter, K.D., Robinet, A., Senechal, N., Ferreira, S.,
1507
1508 561 2015. Impact of the winter 2013-2014 series of severe Western Europe storms on a
1509
1510 562 double-barred sandy coast: Beach and dune erosion and megacusp embayments.
1511
1512 563 *Geomorphology*, 238, 135-148. DOI: 10.1016/j.geomorph.2015.03.006
1513
1514
1515 564 Christie, E.K., Spencer, T., Owen, D., McIvor, A.L., Möller, I., Viavattene, C., 2017.
1516
1517 565 Regional coastal flood risk assessment for a tidally dominant, natural coastal setting:
1518
1519 566 North Norfolk, southern North Sea. *Coastal Engineering*, in press. DOI:
1520
1521 567 10.1016/j.coastaleng.2017.05.003
1522
1523
1524
1525
1526
1527
1528
1529
1530
1531
1532
1533
1534

- 1535
1536
1537 568 Ciavola, P., Ferreira, O., van Dongeren, A., de Vries, J., Armaroli, C., Harley, M., 2015.
1538
1539 569 Prediction of storms impacts on beach and dune systems. In: *Hydrometeorological*
1540
1541 570 *Hazards: Interfacing Science and Policy*. Ed: Philippe Quevauviller, John Wiley & Sons.
1542
1543
1544
1545 571 Clay, P.M., Colburn, L.L., Seara, T., 2016. Social bonds and recovery: An analysis of
1546
1547 572 Hurricane Sandy in the first year after landfall. *Marine Policy*, 74, 334-340. DOI:
1548
1549 573 10.1016/j.marpol.2016.04.049
1550
1551
1552 574 Davidson, M.A., Aarninkhof, S., van Koningsveld, M., Holman, R.A., 2006. Developing
1553
1554 575 coastal video monitoring systems in support of coastal zone management. *Journal of*
1555
1556 576 *Coastal Research*, SI 39, 49-56.
1557
1558
1559
1560 577 Davidson, M.A., van Koningsveld, M., de Kruif, A., Rawson, J., Holman, R., Lamberti, A.,
1561
1562 578 Medina, R., Kroon, A., Aarninkhof, S., 2007. The CoastView project: Developing video-
1563
1564 579 derived Coastal State Indicators in support of coastal zone management. *Coastal*
1565
1566 580 *Engineering*, 54, 463-475. DOI: 10.1016/j.coastaleng.2007.01.007
1567
1568
1569
1570 581 Davidson, M.A., Splinter, K.D., Turner, I.L., 2013. A simple equilibrium model for
1571
1572 582 predicting shoreline change. *Coastal Engineering*, 73, 191-202. DOI:
1573
1574 583 10.1016/j.coastaleng.2012.11.002
1575
1576
1577 584 De Roo, A.P.J., Wesseling, C.G., van Deursen, W.P.A., 2000. Physically base driver basin
1578
1579 585 modelling within a GIS: the LISFLOOD model. *Hydrological Processes*, 14, 1981-1992.
1580
1581 586 DOI: 10.1002/1099-1085(20000815/30)14:11/12<1981::AID-HYP49>3.0.CO;2-F
1582
1583
1584
1585 587 Del Río, L., Plomaritis, T.A., Benavente, J., Valladares, M., Ribera, P., 2012. Thresholds
1586
1587 588 for storm impacts along European coastlines. *Geomorphology*, 143-144, 13-23.
1588
1589 589 DOI:10.1016/j.geomorph.2011.04.048
1590
1591
1592
1593

- Divory, D. and McDougal, W.G., 2006. Response-based coastal flood analysis. *Proceedings of the 30th International Conference on Coastal Engineering*, 5291-5301, ASCE.
- Donnelly, C., 2008. *Coastal Overwash: Processes and Modelling*. PhD Thesis. Lund University, Sweden, 53 pp.
- Dottori, F., Martina, M.L.V., Figueiredo, R., 2016. A methodology for flood susceptibility and vulnerability analysis in complex flood scenarios. *Journal of Flood Risk Management*, DOI: 10.1111/jfr3.12234
- Durán, R., Guillén, J., Ruiz, A., Jiménez, J.A., Sagristà, E., 2016. Morphological changes, beach inundation and overwash caused by an extreme storm on a low-lying embayed beach bounded by a dune system (NW Mediterranean). *Geomorphology*, 274, 129-142. DOI: 10.1016/j.geomorph.2016.09.012
- Ferreira, O., Viavattene, C., Jiménez, J., Bole, A., Plomaritis, T., Costas, S., Smets, S., 2016. CRAF Phase 1, a framework to identify coastal hotspots to storm impacts. *E3S Web Conf.* 7, 11008 (FLOODrisk 2016: 3rd European Conference on Flood Risk Management).
- Fortunato, A.B., Li, K., Bertin, X., Rodrigues, M., Miguez, B.M., 2016. Determination of extreme sea levels along the Iberian Atlantic coast. *Ocean Engineering*, 111, 471-482. DOI:10.1016/j.oceaneng.2015.11.031
- Garcia, T., Ferreira, O., Matias, A., Dias, J.A., 2010. Overwash vulnerability assessment based on long-term washover evolution. *Natural Hazards*, 54, 225-244. DOI: 10.1007/s11069-009-9463-3

- 612 Gouldy, B. and Samuels., P, 2005. Language of Risk – Project Definitions. Report: T32-
613 04-01.Floodsite Project. Available at www.floodsite.net
- 614 Guza, R.T and Inman, D.I., 1975. Edge waves and beach cusps. *Journal of Geophysical*
615 *Research*, 80, 1328-1342. DOI: 10.1029/JC080i021p02997
- 616 Haerens, P., Bolle, A., Trouw, K., Houthuys, R., 2012. Definition of storm thresholds for
617 significant morphological change of the sandy beaches along the Belgian coastline.
618 *Geomorphology*, 143-144, 104-117. DOI:10.1016/j.geomorph.2011.09.015
- 619 Hanslow, D.J., 2007. Beach erosion trend measurement: A comparison of trend
620 indicators. *Journal of Coastal Research*, SI 50, 588-593.
- 621 Hinkel, J., Lincke, D., Vafeidis, A.T., Perrette, M., Nicholls, R.J., Tol, R.S.J., Marzeion, B.,
622 Fettweis, X., Ionescu, C., Levermann, A., 2014. Coastal flood damage and adaptation
623 costs under 21st century sea-level rise, *Proceedings of the National Academy of*
624 *Sciences of the United States of America*, 111, 3292–3297. doi:
625 10.1073/pnas.1222469111
- 626 Holman, R.A., 1986. Extreme value statistics for wave run-up on a natural beach.
627 *Coastal Engineering*, 9, 527–544. DOI: 10.1016/0378-3839(86)90002-5
- 628 Jiménez, A.C., Ávila, J.I.E, Lacouture, M.M.V., Casarín, R., 2016. Classification of beach
629 erosion vulnerability on the Yucatan Coast. *Coastal Management*, 44, 333-349. DOI:
630 10.1080/08920753.2016.1155038
- 631 Judge, E.K., Overton, M.F., Fisher, J.S., 2003. Vulnerability indicators for coastal dunes.
632 *Journal of Waterway, Port, Coastal and Ocean Engineering*, 129, 270-278. DOI:
633 10.1061/(ASCE)0733-950X(2003)129:6(270)

- 634 Kantha, L., 2013. Classification of hurricanes: Lessons from Katrina, Ike, Irene, Isaac and
635 Sandy. *Ocean Engineering*, 70, 124-128. DOI: 10.1016/j.oceaneng.2013.06.007
- 636 Kindsvater, C. and Carter, R., 1957. Discharge characteristics of rectangular thin-plate
637 weirs, *Journal of the Hydraulics Division*, ASCE, 83, 1453/1-1453/36.
- 638 Kriebel, D. and Dean, R.G., 1993. Convolution model for time-dependent beach-profile
639 response. *Journal of Waterway, Port, Coastal and Ocean Engineering*, 119, 204-226.
640 DOI: 10.1061/(ASCE)0733-950X(1993)119:2(204)
- 641 Larson, M., Erikson, L., Hanson, H., 2004. An analytical model to predict dune erosion
642 due to wave impact. *Coastal Engineering*, 51, 675-696. DOI:
643 10.1016/j.coastaleng.2004.07.003
- 644 Link, L.E., 2010. The anatomy of a disaster, an overview of Hurricane Katrina and New
645 Orleans. *Ocean Engineering*, 37, 4-12. DOI: 10-1016/j.oceaneng.2009.09.002
- 646 Long, J.W., de Bakker, A.T.M., Plant, N.G., 2014. Scaling coastal dune elevation changes
647 across storm-impact regimes. *Geophysical Research Letters*, 41.
648 DOI:10.1002/2014GL059616
- 649 Masselink, G. and Hegge, B., 1995. Morphodynamics of meso and macrotidal beaches:
650 examples from central Queensland, Australia. *Marine Geology*, 129, 1-23. DOI:
651 10.1016/0025-3227(95)00104-2
- 652 Masselink, G., Scott, T., Poate, T., Russell, P., Davidson, M., Conley, D., 2016a. The
653 extreme 2013/2014 winter storms: hydrodynamic forcing and coastal response along
654 the southwest coast of England. *Earth Surface Processes and Landforms*, 41, 378-391.
655 DOI: 10.1002/esp.3836

- 656 Masselink, G., Castelle, B., Scott, T., Dodet, G., Suanez, S., Jackson, D., Floc'h, F., 2016b.
- 657 Extreme wave activity during 2013/2014 winter and morphological impacts along the
- 658 Atlantic coast of Europe. *Geophysical Research Letters*, 43, 2135-2143. DOI:
- 659 10.1002/2015GL067492
- 660 Matias, A., Masselink, G., Turner, I., Williams, J.J., Ferreira, Ó., 2011. Detailed analysis
- 661 of overwash on gravel barriers. *Journal of Coastal Research*, SI 64, 10-14.
- 662 Matias, A., Williams, J., Masselink, G., Ferreira, O., 2012. Overwash threshold for gravel
- 663 barriers. *Coastal Engineering*, 63, 48-61. DOI: 10.1016/j.coastaleng.2011.12.006
- 664 Matias, A., Blenkinsopp, C.E., Masselink, G., 2014. Detailed investigation of overwash
- 665 on a gravel barrier. *Marine Geology*. 350, 27-38. DOI: 10.1016/j.margeo.2014.01.009
- 666 Matias, A., Masselink, G., Castelle, B., Blenkinsopp, C.E., Kroon, A., 2016.
- 667 Measurements of morphodynamic and hydrodynamic overwash processes in a large-
- 668 scale wave flume. *Coastal Engineering*, 113, 33-46. DOI:
- 669 10.1016/j.coastaleng.2015.08.005
- 670 Matias, A.. and Masselink, G., 2017. Overwash processes: lessons from fieldwork and
- 671 laboratory experiments. In: *Coastal Storms: Processes and Impacts*. Ed: Paolo Ciavola
- 672 and Giovanni Coco. John Wiley & Sons.
- 673 Mendoza, E.T. and Jiménez, J.A., 2006. Storm-induced beach erosion potential on the
- 674 Catalanian coast. *Journal of Coastal Research*, SI 48, 81-88.
- 675 Neumann, B., Vafeidis, A.T., Zimmermann, J., Nicholls, R.J., 2015. Future Coastal
- 676 Population Growth and Exposure to Sea-Level Rise and Coastal Flooding - A Global
- 677 Assessment. *PLoS ONE*, 10, e0118571.

- 678 Nguyen, T.T.X., Bonetti, J., Rogers, K., Woodroffe, C.D., 2016. Indicator-based
679 assessment of climate-change impacts on coasts: A review of concepts, methodological
680 approaches and vulnerability indices. *Ocean and Coastal Management*, 123, 18-43.
681 DOI: 10.1016/j.ocecoaman.2015.11.022
- 682 Perini, L., Calabrese, L., Salerno, G., Ciavola, P., Armaroli, C., 2016. Evaluation of coastal
683 vulnerability to flooding: comparison of two different methodologies adopted by the
684 Emilia-Romagna region (Italy). *Natural Hazards and Earth Systems Science*, 16, 181-
685 194. DOI: 10.5194/nhess-16-181-2016
- 686 Poelhekke, L., Jäger, W.S, van Dongeren, A., Plomaritis, T.A., McCall, R., Ferreira, O.,
687 2016. Predicting coastal hazards for sandy coasts with a Bayesian Network. *Coastal*
688 *Engineering*, 118, 21-34. DOI: 10.1016/j.coastaleng.2016.08.011
- 689 Poulter, B. and Halpin, P. N., 2008. Raster modelling of coastal flooding from sea-level
690 rise. *International Journal of Geographical Information Science*, 22, 167-182.
691 DOI: 10.1080/13658810701371858
- 692 Ramirez, J.A., Lichter, M., Coulthard, T.J., Skinner, C., 2016. Hyperresolution mapping
693 of regional storm surge and tide flooding: comparison of static and dynamic models,
694 *Natural Hazards*, 82, 571–590. DOI: 10.1007/s11069-016-2198-z
- 695 Rodrigues, B. A., Matias, A., Ferreira, O., 2012. Overwash hazard assessment.
696 *Geologica Acta*, 10, 427-437. DOI: 10.1344/105.000001743
- 697 Roelvink, D., Reniers, A., van Dongeren, A.P., de Vries, J.V.T., McCall, R., Lescinski, J.,
698 2009. Modelling storm impacts on beaches, dunes and barrier islands. *Coastal*
699 *Engineering*, 56, 1133-1152. DOI: 10.1016/j.coastaleng.2009.08.006

1889
1890
1891 700 Sallenger, A.H., 2000. Storm impact scale for barrier islands. *Journal of Coastal*
1892
1893 701 *Research*, 16, 890-895.
1894
1895
1896 702 Sánchez-Arcilla, A., Jiménez, J.A., Peña, C., 2009. Wave-induced morphodynamic risks.
1897
1898
1899 703 Characterization of extremes. *Coastal Dynamics 2009*, World Scientific (CD), paper 127.
1900
1901
1902 704 Sekovski, I., Armaroli, C., Calabrese, L., Mancini, F., Stecchi, F., Perini, L., 2015. Coupling
1903
1904 705 scenarios of urban growth and flood hazards along the Emilia-Romagna coast (Italy).
1905
1906 706 *Natural Hazards and Earth System Sciences*, 15, 2331-2346, DOI: 10.5194/nhess-15-
1907
1908 707 2331-2015
1909
1910
1911 708 Silveira, T.M., Taborda, R., Carapuço, M.M., Andrade, C., Freitas, M.C., Duarte, J.F.,
1912
1913
1914 709 Psuty, N.P., 2016. Assessing the extreme overwash regime along an embayed urban
1915
1916 710 beach. *Geomorphology*, 274, 64-77. DOI: 10.1016/j.geomorph.2016.09.007
1917
1918
1919 711 Smallegan, S.M., Irish, J.L., van Dongeren, A.R., den Bieman, J.P., 2016. *Morphological*
1920
1921 712 *response of a sandy barrier island with a buried seawall during Hurricane Sandy.*
1922
1923 713 *Coastal Engineering*, 110, 102-110. DOI: 10.1016/j.coastaleng.2016.01.005
1924
1925
1926 714 Stockdon, H.F., Holman, R.A., Howd, P.A., and Sallenger, A.H., 2006. Empirical
1927
1928 715 parameterization of setup, swash and run-up. *Coastal Engineering*, 53, 573-588.
1929
1930 716 DOI: 10.1016/j.coastaleng.2005.12.005
1931
1932
1933 717 Stockdon, H.F., Sallenger Jr, A.H., Holman, R.A., Howd, P.A., 2007. A simple model for
1934
1935 718 the spatially-variable coastal response to hurricanes. *Marine Geology*, 238, 1-20.
1936
1937
1938 719 DOI:10.1016/j.margeo.2006.11.004
1939
1940
1941
1942
1943
1944
1945
1946
1947

1948
1949
1950
1951
1952
1953
1954
1955
1956
1957
1958
1959
1960
1961
1962
1963
1964
1965
1966
1967
1968
1969
1970
1971
1972
1973
1974
1975
1976
1977
1978
1979
1980
1981
1982
1983
1984
1985
1986
1987
1988
1989
1990
1991
1992
1993
1994
1995
1996
1997
1998
1999
2000
2001
2002
2003
2004
2005
2006

720 Trifonova, E.V., Valchev, N.N., Andreeva, N.K., Eftimova, P.T., 2012. Critical storm
721 thresholds for morphological changes in the western Black Sea coastal zone.
722 *Geomorphology*, 143–144, 81–94. DOI:10.1016/j.geomorph.2011.07.036

723 Valchev, N., Andreeva, N., Eftimova, P., Prodanov, B., Kotsev, I., 2016. Assessment of
724 vulnerability to storm induced flood hazard along diverse coastline settings. *E3S Web*
725 *Conference* 7, 10002. FLOODrisk 2016 - 3rd European Conference on Flood Risk
726 Management.

727 van Koningsveld, M., Davidson, M.A., Huntley, D.A., 2005. Matching science with
728 coastal management needs: The search for appropriate coastal state indicators.
729 *Journal of Coastal Research*, 21, 399-411. DOI: 10.2112/03-0076.1

730 van Verseveld, H.C.W., van Dongeren, A.R., Plant, N.G., Jäger, W.S., den Heijer, C.,
731 2015. Modelling multi-hazard hurricane damages on an urbanized coast with a
732 Bayesian Network approach. *Coastal Engineering*, 103, 1-14. DOI:
733 10.1016/j.coastaleng.2015.05.006

734 Vousdoukas, M.I., Voukouvalas, E., Mentaschi, L., Dottori F., Giardino, A., Bouziotas, D.,
735 Bianchi, A., Salamon, P., Feyen, L., 2016. Developments in large-scale coastal flood
736 hazard mapping. *Natural Hazards Earth System Science*, 16, 1841-1853. DOI:
737 10.5194/nhess-2016-124.

738 Williams, J.J., Masselink, G., Buscombe, D., Turner, I., Matias, A., Ferreira, Ó., Metje, N.,
739 Coates, L., Chapman, D., Bradbury, A., Albers, A., Pan, S., 2009. BARDEX (Barrier
740 Dynamics Experiment): taking the beach into the laboratory. *Journal of Coastal*
741 *Research*, SI 56: 158-162.

2007		
2008		
2009	742	Wright, L.D. and Short, A.D., 1984. Morphodynamic variability of surf zones and
2010		
2011	743	beaches: a synthesis. <i>Marine Geology</i> , 56, 93-118. DOI: 10.1016/0025-3227(84)90008-
2012		
2013		
2014	744	2
2015		
2016		
2017		
2018		
2019		
2020		
2021		
2022		
2023		
2024		
2025		
2026		
2027		
2028		
2029		
2030		
2031		
2032		
2033		
2034		
2035		
2036		
2037		
2038		
2039		
2040		
2041		
2042		
2043		
2044		
2045		
2046		
2047		
2048		
2049		
2050		
2051		
2052		
2053		
2054		
2055		
2056		
2057		
2058		
2059		
2060		
2061		
2062		
2063		
2064		
2065		

Table I. Synthesis of process-based indicators by hazard, including calculation methods, input parameters, area of application and potential visual expression. OD – Overwash depth; OE – Overwash extent; FD – Flood depth; FE – Flood extent; SBR – Shoreline/berm retreat; DFR – Dune foot retreat; VE – Vertical erosion. The numbers in brackets refer to works where the indicators application/details can be found.

Hazard	Indicator	Method	Input parameters	Application [References]	Visual expression
Overwash	Overwash potential	Runup formulation (e.g. Holman, Stockdon)	Hs, Tp, sea level, beach face slope, dune crest height	Natural beaches/dunes [1-12]	Linear (along dune crest)
	Overwash depth	Runup formulation (e.g. Holman, Stockdon) + Donnelly formulation for depth decrease	Hs, Tp, sea level, beach face slope, dune crest height, backbarrier topography, overwash lens angle, backbarrier slope	Natural beaches/dunes/backbarriers [13-15]	2D with 3D possibility in association with OE
		Numerical models (e.g. XBeach)	Nearshore wave conditions (Hs, Tp, direction); topo-bathymetry	Natural beaches/dunes/backbarriers [16, 17]	2D with 3D possibility in association with OE
Inundation	Overwash extent	Donnelly Washover extent Formulation/XBeach	Hs, Tp, sea level, beach face slope, dune crest height, backbarrier topography, overwash lens angle, backbarrier slope/Nearshore wave conditions (Hs, Tp, direction); topo-bathymetry	Natural beaches/dunes/backbarriers [13-15, 18]	2D with 3D possibility in association with OD
	Flood depth/extent	Bathtub or tilted bathtub	Total sea level (tide + surge); Topography	Coastal areas with low morphological complexity [19-26]	2D with 3D possibility in association with FE/FD
	Flood depth/extent	Numerical models (e.g. LISFLOOD) or semi-static approaches	Water discharge/level; Topography	Low to complex hinterland morphologies [19, 24, 26]	3D
	Overflowing discharge volume	Numerical models (e.g. LISFLOOD) or semi-static approaches	Water discharge/level; Topography	Low to complex hinterland morphologies [19, 26]	3D

Erosion	Shoreline/berm retreat; Dune foot retreat;	Convolution model; Larson's model; Erosion structural function	Nearshore wave conditions (Hs, Tp, direction); topo-bathymetry	Natural beaches/dunes [3, 13, 27-32]	SBR and DFR - 2D; VE - 3D
	Vertical erosion	Numerical models (e.g. XBeach)			

[1] Almeida et al., 2012; [2] Armaroli et al., 2012; [3] Bosom and Jiménez, 2011; [4] Del Rio et al., 2012; [5] Duran et al., 2016; [6] Haerens et al., 2012; [7] Long et al., 2014; [8] Matias et al., 2014; [9] Rodrigues et al., 2012; [10] Silveira et al., 2017; [11] Stockton et al., 2007; [12] Trifonova et al., 2012; [13] Ferreira et al., 2016; [14] Christie et al., 2017; [15] Valchev et al., 2016; [16] Poelhekke, et al., 2016; [17] van Verseveld , et al., 2015; [18] Garcia et al., 2010; [19] Breilh et al., 2013; [20] Dottori et al., 2016; [21] Hinkel, et al., 2014; [22] Perini et al., 2016; [23] Poulter and Halpin, 2008; [24] Ramirez et al., 2016; [25] Sekovski et al., 2015; [26] Vousedoukas et al., 2016; [27] Almeida et al., 2011; [28] Callaghan et al., 2008; [29] Ciavola et al., 2015; [30] Davidson et al., 2006; [31] Jiménez et al., 2016; [32] Mendoza and Jiménez, 2006; [33] McCall et al., 2010; [34] Smollegan et al., 2016; [35] van Verseveld et al., 2015.

Table II. Comparison between computation type, longshore variability, comparability among coastal areas and cross-shore expression for selected geo, driver and process-based indicators.

Indicator type	Indicator name	Computation type	Longshore variability	Hazard comparability between coastal areas	Cross-shore hazard expression
Geoindicators	Shoreline position	DM/CE	Yes	Reduced	No
	Barrier/beach elevation	DM/CE	Yes	Reduced	No
	Beach/coastal slope	DM/CE	Yes	Reduced	No
	Erosion rate	CE/F/M	Yes	High	Yes
Driver-based indicators	Wave height	I/H	Reduced/Yes ^a	Reduced	No
	Tidal range	I/H	Reduced	Reduced	No
	Surge height	I/H	Reduced	Reduced	No
Process-based indicators	Overwash depth	F/M	Yes	High	Yes
	Overwash potential	F/M	Yes	High	No
	Overwash extent	F/M	Yes	High	Yes
Process-based indicators	Flood depth	F/M	Yes	High	Yes
	Flood extent	F/M	Yes	High	Yes
Process-based indicators	Shoreline/berm retreat	F/M	Yes	High	Yes
	Dune foot retreat	F/M	Yes	High	Yes
	Vertical erosion	F/M	Yes	High	Yes

^a requires wave propagation models to include detailed longshore variability near the coastline;

DM – direct measurement; CE – cartographic extraction; I – instrumental; H – hindcast; F – formulation; M – model.